

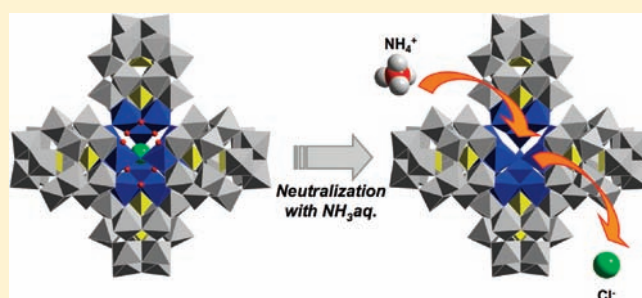
Encapsulation of Anion/Cation in the Central Cavity of Tetrameric Polyoxometalate, Composed of Four Trititanium(IV)-Substituted α -Dawson Subunits, Initiated by Protonation/Deprotonation of the Bridging Oxygen Atoms on the Intramolecular Surface

Yoshitaka Sakai, Shuji Ohta, Yukihiro Shintoyo, Shoko Yoshida, Yuhki Taguchi, Yusuke Matsuki, Satoshi Matsunaga, and Kenji Nomiya*

Department of Chemistry (old name Department of Materials Science), Faculty of Science, Kanagawa University, Hiratsuka, Kanagawa 259-1293, Japan

Supporting Information

ABSTRACT: Preparation and structural characterization of a novel polyoxometalate (POM), $[(P_2W_{15}Ti_3O_{60.5})_4(NH_4)]^{35-}$ **1**, i.e., an encapsulated NH_4^+ cation species in the central cavity of a tetramer (called the Dawson tetramer) constituted by trititanium(IV)-substituted α -Dawson POM substructure, are described. POM **1** was synthesized by several different methods and unequivocally characterized by complete elemental analysis, thermogravimetric and differential thermal analysis (TG/DTA), FTIR spectroscopy, solution ($^{15}N\{^1H\}$, ^{31}P , ^{183}W) NMR spectroscopy, and X-ray crystallography. First, POM **1** was synthesized by a reaction of NH_4Cl in aqueous solution with a precursor, which was derived by thermal treatment of a monomeric triperoxotitanium(IV)-substituted Dawson POM, $[\alpha-1,2,3-P_2W_{15}(TiO_2)_3O_{56}(OH)_3]^9-$ **2**, for 3 h in an electric furnace at 200 °C. The encapsulated NH_4^+ cation in **1** was confirmed by $^{15}N\{^1H\}$ NMR measurement and X-ray crystallography. As another synthesis of **1**, a direct exchange of the Cl^- anion encapsulated in $[\{\alpha-1,2,3-P_2W_{15}Ti_3O_{57.5}(OH)_3\}_4Cl]^{25-}$ **3** with the NH_4^+ cation was attained by neutralizing an aqueous solution containing **3** with the addition of aqueous NH_3 (the initial pH of ca. 2–2.5 was changed to 6.4), followed by adding NH_4Cl . It has been clarified that the conditions as to whether the anion or the cation is encapsulated in the central cavity of the Dawson tetramer were significantly related to the protonation/deprotonation of the bridging oxygen atoms on the intramolecular surface, Ti–O–Ti/Ti–OH–Ti sites constituting the Dawson subunits.



INTRODUCTION

Polyoxometalates (POMs) are molecular metal–oxide clusters, which have attracted considerable attention in the fields of catalysis, medicine, surface science, and materials science, since POMs are often considered to be molecular analogues of metal oxides in terms of structural analogy.¹ From a structural viewpoint, POM-based giant molecules have recently received much attention.² In fact, many POM-based giant molecules have been prepared, through self-assembly of Keggin or Dawson lacunary units or other substructure units, e.g., as $[As^{III}_{12}Ce^{III}_{16}(H_2O)_{36}W_{148}O_{524}]^{76-}$,^{2a} $[\{Sn(CH_3)_2(H_2O)\}_2]_{24}\{Sn(CH_3)_2\}_{12}(A-XW_9O_{34})_{12}]^{36-}$ ($X = P, As$),^{2b} $[Gd_6As_6W_{65}O_{229}(OH)_4(H_2O)_{12}(OAc)_2]^{38-}$,^{2c} $[Yb_{10}As_{10}W_{88}O_{308}(OH)_8(H_2O)_{28}(OAc)_4]^{40-}$,^{2c} $[W_{72}Mn^{III}_{12}O_{268}X_7]^{40-}$ ($X = Si, Ge$),^{2d,e} $[(H_2P_2W_{15}O_{56})_4\{Mo_2O_2S_2(H_2O)_2\}_4\{Mo_4S_4O_4(OH)_4(H_2O)\}_2]^{28-}$,^{2f} $[(UO_2)_{12}(\mu_3-O)_4(\mu_2-H_2O)_{12}(P_2W_{15}O_{56})_4]^{32-}$,^{2g} $[KFe_{12}(OH)_{18}(\alpha-1,2,3-P_2W_{15}O_{56})_4]^{29-}$,^{2h} and $[Cu_{20}Cl(OH)_{24}(H_2O)_{12}(P_8W_{48}O_{184})]^{25-}$.²ⁱ The two compounds in refs 2g and 2h possess the tetrahedral structure based on the Dawson tetramer. A number of polyoxomolybdate-based

giant molecules have also been reported as mixed valence molybdates by Müller's group,^{1ij} the formation of which has involved a reduction process of a part of molybdates in aqueous media.

Site-selective substitution of the W^{VI} atoms in POMs with Ti^{IV} atoms is particularly interesting, because of the formation of multicenter active sites with corner- or edge-sharing TiO_6 octahedra and, also, generation of oligomeric species through Ti–O–Ti bonds.^{3,4} The ionic radius of Ti^{IV} (0.75 Å) is close to that of W^{VI} (0.74 Å), suggesting that Ti^{IV} should fit nicely into the POM framework. However, there is a significant consequence in terms of oligomeric Ti–O–Ti anhydride formation resulting from substitution by several Ti^{IV} atoms. As a matter of fact, many examples of Keggin POM-based oligomeric species are reported.^{3e–r}

On the other hand, fewer examples of oligomeric species of Ti^{IV} -substituted Dawson POMs are reported. For example, the dimeric Dawson POM bridged by two $Ti(ox)_2$ groups

Received: February 18, 2011

Published: June 15, 2011

(H₂Ox = oxalic acid), [P₂W₁₆Ti₂O₆₂{μ-Ti(C₂O₄)₂}]₂^{20-4a}, dilacunary Dawson sandwich complex, (NH₄)₁₄[P₂W₁₅O₅₅Ti(OH)₂·nH₂O]_{4b} and its free acid form, H₈[Ti₂{P₂W₁₅O₅₄(OH)₂]₂·3H₂O,^{4c} and the two mono-Ti^{IV}-substituted Dawson POM dimers, i.e., K₁₄[(α₂-P₂W₁₇TiO₆₁)₂(μ-O)]·17H₂O^{4d} and H₁₃[(α₂-P₂W₁₇TiO₆₁)(α₂-P₂W₁₇TiO₆₁H)(μ-O)]·5.5H₂O,^{4d} have been reported. Furthermore, tetramers composed of tri-Ti^{IV}-substituted Dawson POM substructures have also been isolated as two giant “tetrapod”-shaped POMs, i.e., tetrameric Ti–O–Ti-bridged anhydride forms without bridging μ₃-Ti(H₂O)₃ octahedral groups (called the nonbridging Dawson tetramer) and the species with bridging μ₃-Ti(H₂O)₃ groups (called the bridging Dawson tetramer), both of which have an encapsulated Cl[−] anion in the central cavity, such as [{α-1,2,3-P₂W₁₅Ti₃O_{57.5}(OH)₃]₄Cl]²⁵⁻ (3)^{5b-d} and [{α-1,2,3-P₂W₁₅Ti₃O₅₉(OH)₃]₄{μ₃-Ti(H₂O)₃]₄Cl]²¹⁻ (4).^{5a,d} As to 4, we have recently obtained three bridging Dawson tetramers with different anions encapsulated, [{α-1,2,3-P₂W₁₅Ti₃O₅₉(OH)₃]₄{μ₃-Ti(H₂O)₃]₄X]²¹⁻ (X = Br, I, NO₃).^{5e} As a related compound, the monomeric triperoxotitanium(IV)-substituted Dawson POM [α-1,2,3-P₂W₁₅(TiO₂)₃O₅₆(OH)₃]⁹⁻ (2) has been derived from a reaction of 4 with aqueous hydrogen peroxide, but not from a reaction of 3.^{5d} Preliminary experiments have shown that the monomeric peroxy-compound 2 can be used as a building block for preparation of the two giant “tetrapod”-shaped POMs, 3 and 4, by killing the coordinating peroxy group thermally or chemically using NaHSO₃.^{5d} In this work, we first synthesized the encapsulated NH₄⁺ cation species in the nonbridging Dawson tetramer, [(α-1,2,3-P₂W₁₅Ti₃O_{60.5})₄(NH₄)]³⁵⁻ (1). The encapsulated NH₄⁺ cation was confirmed by ¹⁵N{¹H} NMR measurement and X-ray crystallography. Furthermore, using 3, we also realized a direct exchange of the Cl[−] anion encapsulated in the central cavity with the NH₄⁺ cation. The conditions as to whether the anion or the cation was encapsulated therein were found to be significantly related to the protonation of the surface Ti–O–Ti sites within the Dawson subunits. The protonated species of the Ti–O–Ti sites resulted in encapsulation of the anion in the central cavity, while the deprotonated species led to encapsulation of the cation therein.

Herein, we report full details of the synthesis and structure of the novel nonbridging Dawson tetramer with an encapsulated NH₄⁺ cation, (NH₄)₂₇Na₈[(P₂W₁₅Ti₃O_{60.5})₄(NH₄)]₄·ca. 90H₂O (NH₄Na-1) and (NH₄)₂₄Na₇K₄[(P₂W₁₅Ti₃O_{60.5})₄(NH₄)]₄·ca. 50H₂O (NH₄NaK-1). [Note: the polyoxoanion moiety in NH₄Na-1 and NH₄NaK-1 is abbreviated simply as L.]

EXPERIMENTAL SECTION

Materials. The following reactants were used as received: NH₄Cl, ¹⁵NH₄Cl (Wako); D₂O (Isotec). The trilacunary Dawson POM, Na₁₂[P₂W₁₅O₅₆]₄·nH₂O (n = 19, 25), was synthesized via pure K₆[α-P₂W₁₈O₆₂]₄·nH₂O (n = 13, 14) prepared by modification of the literature,^{6a,b} and characterized by solid-state CPMAS ³¹P and solution ³¹P NMR, FTIR, and TG/DTA (see Supporting Information). Solution ³¹P NMR of a freshly prepared D₂O solution was in excellent accord with the literature data.^{6c-e} Syntheses and characterizations of the three POM precursors [the monomeric, peroxy-titanium(IV)-containing species Na₉[P₂W₁₅(TiO₂)₃O₅₆(OH)₃]₄·14H₂O (Na-2), the nonbridging Dawson tetramer with an encapsulated Cl[−] ion, Na₂₁K₄[(P₂W₁₅Ti₃O_{57.5}(OH)₃]₄Cl]₄·70H₂O (NaK-3), and the bridging Dawson tetramer with an encapsulated Cl[−] ion, Na₁₉H₂[(α-1,2,3-P₂W₁₅Ti₃O₅₉(OH)₃]₄{μ₃-Ti(H₂O)₃]₄Cl]₄·124H₂O (NaH-4)] have been reported elsewhere.^{5a,b,d}

Instrumentation/Analytical Procedures. Complete elemental analysis was carried out by Mikroanalytisches Labor Pascher (Remagen, Germany). A sample was dried at room temperature under 10^{−3}–10^{−4} Torr overnight before the complete elemental analysis. Infrared spectra were recorded on a Jasco 4100 FTIR spectrometer in KBr disks at room temperature. Thermogravimetric (TG) analyses and differential thermal analyses (DTA) were acquired using a Rigaku Thermo Plus 2 series TG/DTA TG 8120 instrument. TG/DTA measurement was run under air with a temperature ramp of 4 °C/min between 20 and 500 °C.

³¹P NMR (161.70 MHz) spectra in a D₂O solution were recorded in 5-mm outer diameter tubes on a JEOL JNM-EX 400 FT-NMR spectrometer with a JEOL EX-400 NMR data processing system. ³¹P NMR spectra were measured in a D₂O solution with reference to an external standard of 25% H₃PO₄ in H₂O in a sealed capillary. The ³¹P NMR data with the usual 85% H₃PO₄ reference were shifted to +0.544 ppm from our data. Chemical shifts were reported as negative for resonances upfield from 25% H₃PO₄ (δ 0). ¹⁸³W NMR (16.50 MHz) spectra were recorded in 10-mm outer diameter tubes on a JEOL NM40T10L low-frequency tunable probe and a JEOL EX 400 NMR data processing system. ¹⁸³W NMR spectra measured in D₂O were referenced to an external standard of a saturated Na₂WO₄–D₂O solution. The ¹⁸³W NMR signals were shifted to −0.787 ppm by using a 2 M Na₂WO₄ solution as a reference instead of a saturated Na₂WO₄ solution. Chemical shifts were reported as negative for resonances upfield from Na₂WO₄ (δ 0). ¹⁵N{¹H} NMR (50.00 MHz) spectra in a D₂O solution were recorded in 5-mm outer diameter tubes on a JEOL ECP-500 FT-NMR spectrometer with a JEOL ECP-500 NMR data processing system. The ¹⁵N{¹H} NMR spectrum was measured in a D₂O solution with reference to an external standard of NH₄NO₃ in a D₂O solution. Chemical shifts were reported as positive for resonances downfield from NH₄NO₃ (δ 30.0, NH₄⁺).

Synthesis. (NH₄)₂₇Na₈[(α-1,2,3-P₂W₁₅Ti₃O_{60.5})₄(NH₄)]₄·ca. 90H₂O (NH₄Na-1). Solid Na₉[P₂W₁₅(TiO₂)₃O₅₆(OH)₃]₄·14H₂O (Na-2) was treated for 3 h in an electric furnace at 200 °C. The resulting white yellow powder (0.5 g) was dissolved in 12 mL of water, and then stirred for 30 min. To the yellow clear solution was added 0.12 g (2.24 mmol) of NH₄Cl, followed by stirring for 30 min in a water bath at about 80 °C. The clear yellow solution was left to stand at 30 °C in a water bath for 1 day. Additionally, the solution was left to stand at 27 °C in a water bath for 1 day. The colorless needle crystals formed were collected on a membrane filter (JG 0.2 μm), washed with EtOH (10 mL × 3) and then Et₂O (50 mL × 3), and dried in vacuo for 2 h. The crystals obtained in 54.0% (0.27 g scale) yield were soluble in water and insoluble in EtOH and Et₂O. Found: H, 0.93; N, 2.26; Na, 1.08; P, 1.47; W, 66.1; Ti, 3.43; O, 24.7; Cl, <0.1; total 99.97%. Calcd for H₁₄₆N₂₈Na₈P₈W₆₀Ti₁₂O₂₅₉ or (NH₄)₂₇Na₈[(P₂W₁₅Ti₃O_{60.5})₄(NH₄)]₄·17H₂O: H, 0.88; N, 2.35; Na, 1.10; P, 1.48; W, 65.97; Ti, 3.44; O, 24.78%. A weight loss of 6.64% (weakly solvated or adsorbed water) was observed during the course of drying at room temperature at 10^{−3}–10^{−4} Torr overnight before analysis, suggesting the presence of 66 water molecules. TG/DTA under atmospheric conditions (Figure S1): a weight loss of 9.18% below 200 °C was observed with endothermic peaks at 40.7, 64.0, 98.0, 121.9, and 183.0 °C; calcd 9.17% for x = 92 in (NH₄)₂₇Na₈[(P₂W₁₅Ti₃O_{60.5})₄(NH₄)]₄·xH₂O. IR(KBr) (polyoxometalate region): 1400 s, 1086 s, 1007 w, 943 s, 912 s, 831 s, 785 s, 687 vs, 600 m, 565 m, 526 m, 480 w, 465 w, 449 w, 403 w cm^{−1}. ³¹P NMR (27.4 °C, D₂O): δ −7.15, −14.23. ³¹P NMR (23.5 °C, 0.1 M HCl aq): δ −7.72, −14.05. ¹⁸³W NMR (14.0 °C, D₂O): δ −154.2 (3 W × 4), −184.3 (6 W × 4), −224.5 (6 W × 4). ¹⁵N{¹H} NMR (35 °C, D₂O): δ 29.89 (counteraction), 35.45 (encapsulated cation). ¹⁵N{¹H} NMR measurement was performed for the ¹⁵N-enriched sample prepared by using ¹⁵NH₄Cl in the above synthesis.

Synthesis of (NH₄)₂₄Na₇K₄[(α-1,2,3-P₂W₁₅Ti₃O_{60.5})₄(NH₄)]₄·ca. 50H₂O (NH₄NaK-1) Using Na₂₁K₄[(α-1,2,3-P₂W₁₅Ti₃O_{57.5}(OH)₃]₄Cl]₄·70H₂O (NaK-3): Exchange of the Encapsulated Chloride Ion with an Ammonium Ion. The

pH of a solution (pH 2–2.5) of $\text{Na}_{21}\text{K}_4[\{\text{P}_2\text{W}_{15}\text{Ti}_3\text{O}_{57.5}(\text{OH})_3\}_4\text{Cl}]\cdot 70\text{H}_2\text{O}$ (**NaK-3**, 2.0 g, 0.11 mmol) dissolved in 40 mL of water was adjusted to 6.4 by adding 3% aqueous NH_3 . To the colorless clear solution, 0.48 g (8.97 mmol) of NH_4Cl was added, followed by stirring for 30 min in a water bath at 80 °C. The colorless clear solution was allowed to stand overnight at 35 °C. The white crystalline powder precipitated was collected on a membrane filter (JG 0.2 μm), washed with EtOH (30 mL \times 3) and then Et₂O (50 mL \times 3), and dried in vacuo for 2 h. The white powder obtained in 45.2% (0.89 g scale) yield was soluble in water and insoluble in EtOH and Et₂O. Found: H, 0.94; N, 1.62; Na, 0.78; K, 0.66; P, 1.53; W, 66.2; Ti, 3.40; O, 24.7; Cl, 0.016; total 99.85%. Calcd for $\text{H}_{130}\text{N}_{25}\text{Na}_7\text{K}_4\text{P}_8\text{W}_{60}\text{Ti}_{12}\text{O}_{257}$ or $(\text{NH}_4)_{24}\text{Na}_7\text{K}_4[(\text{P}_2\text{W}_{15}\text{Ti}_3\text{O}_{60.5})_4(\text{NH}_4)]\cdot 15\text{H}_2\text{O}$: H, 0.78; N, 2.09; Na, 0.96; K, 0.93; P, 1.48; W, 65.80; Ti, 3.43; O, 24.53%. A weight loss of 3.50% (weakly solvated or adsorbed water) was observed during the course of drying at room temperature at 10^{-3} – 10^{-4} Torr overnight before analysis, suggesting the presence of 34 water molecules. TG/DTA under atmospheric conditions (Figure S2): a weight loss of 5.21% below 200 °C was observed with an endothermic peak at 57.1 °C; calcd 5.18% for $x = 50$ in $(\text{NH}_4)_{24}\text{Na}_7\text{K}_4[(\text{P}_2\text{W}_{15}\text{Ti}_3\text{O}_{60.5})_4(\text{NH}_4)]\cdot x\text{H}_2\text{O}$. IR(KBr) (polyoxometalate region): 1401 s, 1086 s, 1008 w, 944 s, 914 s, 831 s, 786 s, 688 vs, 598 m, 567 m, 526 m, 472 w, 405 w cm^{-1} . ³¹P NMR (22.5 °C, D₂O): δ –7.12, –14.25.

We obtained the crystalline sample of **NH₄NaK-1** and tried a single crystal structural analysis. However, we have not obtained good data.

When NaOH, instead of aqueous NH_3 , was used to deprotonate all sodium salt of **3** in the workup, Na⁺ ion is surely encapsulated. [Note: Solid sample of such a compound was difficult to isolate because it was highly soluble in water.] However, there are some problems in the use of NaOH or KOH for the compounds with mixed counterions such as **NaK-3**, because encapsulation significantly depends upon the interaction between counteranion and POM anion. The present workup using aqueous NH_3 and NH_4Cl is also concerned with the solubility in water.

Control Experiment 1: Preparation of **1** Using the Monomeric Trititanium(IV)-Substituted Dawson POM, $[\alpha\text{-}1,2,3\text{-P}_2\text{W}_{15}\text{Ti}_3\text{O}_{62}]^{12-}$ (**5**), Prepared by Hydrolysis of the Bridging Dawson Tetramer with an Encapsulated Chloride Ion (**4**).

(1) For the synthesis of $\text{Na}_{12}[\text{P}_2\text{W}_{15}\text{Ti}_3\text{O}_{62}]\cdot 28\text{H}_2\text{O}$ (**Na-5**), the monomeric form **5** of the trititanium(IV)-substituted Dawson POM cannot be derived from a direct reaction of the trilacunary Dawson species $[\text{P}_2\text{W}_{15}\text{O}_{56}]^{12-}$ with Ti source, but it can be prepared by hydrolysis of the bridging Dawson tetramer with an encapsulated Cl[−] ion **4**. The pH of a solution of $\text{Na}_{19}\text{H}_2[\{\alpha\text{-}1,2,3\text{-P}_2\text{W}_{15}\text{Ti}_3\text{O}_{59}(\text{OH})_3\}_4\{\mu_3\text{-Ti}(\text{H}_2\text{O})_3\}_4\text{Cl}]\cdot 124\text{H}_2\text{O}$ (**NaH-4**, 4.8 g, 0.253 mmol) dissolved in 20 mL of water was adjusted to 9.0 by adding 1 M NaOH aqueous solution. [Note: It took more than 3 h to stabilize and maintain the pH at 9.0 by adding 1 M NaOH aqueous solution.] To the colorless clear solution was added 8.0 g (0.137 mol) of NaCl, followed by stirring for 1 h. The white powder precipitated was collected on a membrane filter (JG 0.2 μm), washed with EtOH (30 mL \times 3) and then Et₂O (50 mL \times 3), and dried in vacuo for 2 h. The white powder obtained in 41.7% (2.0 g scale) yield was soluble in water and insoluble in EtOH and Et₂O. TG/DTA under atmospheric conditions: a weight loss of 10.75% below 307.6 °C was observed with endothermic peaks at 43.3 and 75.4 °C and an exothermic peak at 481.8 °C; calcd 10.65% for $x = 28$ in $\text{Na}_{12}[\text{P}_2\text{W}_{15}\text{Ti}_3\text{O}_{62}]\cdot x\text{H}_2\text{O}$. IR(KBr) (polyoxometalate region): 1631 s, 1088 s, 1051 m, 1014 m, 941 vs, 914 vs, 825 vs, 742 vs, 599 s, 562 s, 525 s, 463 s cm^{-1} . [Note: No Ti–O–Ti vibration band of inter-Dawson units, usually observed in the range 690–650 cm^{-1} as prominent bands in the Dawson tetramers, indicates that this compound is a monomer.] ³¹P NMR (22.9 °C, D₂O): δ –4.94, –14.61.

(2) For the synthesis of the ammonium sodium salt of **1** from the monomer **Na-5**, NH_4Cl (0.06 g, 1.12 mmol) was added to a stirred

solution (pH 9.9) of the monomer (**Na-5**, 0.50 g, 0.11 mmol) dissolved in 12 mL of water. The pH of the solution (pH 8.4) was adjusted to 6.0 using 0.1 M aqueous HCl, followed by stirring for 30 min in a water bath at 80 °C. The solution was evaporated until white powder deposited with a rotary evaporator at 30 °C. After adding 1 mL of water, the white powder was dissolved by further stirring in a water bath at 35 °C. On cooling gradually the solution from 35 °C to room temperature, colorless needle crystals deposited, which were collected on a membrane filter (JG 0.2 μm), washed with EtOH (10 mL \times 3) and Et₂O (50 mL \times 3), and dried in vacuo for 3 h. White powder of the ammonium sodium salt of **1**, obtained in 14.3% (0.067 g scale) yield, was soluble in water and insoluble in EtOH and Et₂O. TG/DTA under atmospheric conditions (Figure S3): a weight loss of 9.7% below 500 °C was observed with an endothermic peak at 48.4 °C. The formula of the ammonium sodium salt of **1** was tentatively determined on the basis of elemental analysis and TG/DTA as $(\text{NH}_4)_y\text{Na}_{35-y}[(\alpha\text{-}1,2,3\text{-P}_2\text{W}_{15}\text{Ti}_3\text{O}_{60.5})_4(\text{NH}_4)]\cdot 70\text{H}_2\text{O}$ ($y = 20\text{--}22$). IR(KBr) (polyoxometalate region): 1620 w, 1407 w, 1086 m, 1008 w, 944 s, 914 m, 892 m, 829 s, 779 s, 683 vs, 599 m, 566 m, 524 m, 468 m cm^{-1} . ³¹P NMR (21.5 °C, D₂O): δ –7.21, –14.20.

Control Experiment 2: In-Situ-Generation of the Nonbridging Dawson Tetramer with an Encapsulated Sodium Ion. In a fume hood, ca. 0.1 mL (ca. 0.91 mmol) of TiCl_4 was added to 20 mL of water in an ice bath. To this mixture was added 1.25 g (0.29 mmol) of solid $\text{Na}_{12}[\text{P}_2\text{W}_{15}\text{O}_{56}]\cdot 19\text{H}_2\text{O}$ (see Materials), followed by stirring for 10 min. The pH of the solution was adjusted to 6.6 by adding solid Na_2CO_3 , followed by stirring overnight. The ³¹P NMR of the solution was measured: –7.45, –14.21 ppm (main peaks due to the encapsulated Na⁺ species in the Dawson tetramer) and –4.98, –14.68 ppm (minor peaks due to the monomeric trititanium(IV)-substituted Dawson POM species). Solid sample of the sodium salt with the encapsulated Na⁺ ion was not isolated because of its high solubility. Preliminary data have shown that the ³¹P NMR in D₂O of the in-situ-generated and/or isolated nonbridging Dawson tetramers are significantly changed by encapsulated ions: for NH_4^+ ion (δ ca. –7.14, –14.21), Na⁺ ion (δ ca. –7.42, –14.15), K⁺ ion (δ –7.39, –14.15), Cl[−] (δ –7.62, –13.93).

X-ray Crystallography. A colorless needle crystal of **NH₄Na-1** (0.22 \times 0.08 \times 0.06 mm³) was surrounded by liquid paraffin (Paratone-N) to prevent its degradation. Data collection was done by a Bruker SMART APEX CCD diffractometer at 90 K in a range $1.94^\circ < 2\theta < 56.96^\circ$. The intensity data were automatically corrected for Lorentz and polarization effects during integration. The structure was solved by direct methods (program SHELXS-97)^{7a} followed by subsequent difference Fourier calculation and refined by a full-matrix least-squares procedure on F^2 (program SHELXL-97).^{7b} Absorption correction was performed with SADABS (empirical absorption correction).^{7c} The composition and formula of the POM containing many counterions and many hydrated water molecules have been determined by complete elemental analysis and TG/DTA analysis. Refinements of the positions of many counterions and many solvent molecules in the POM are limited because of their disorder. We can reveal only the molecular structure of the POM, but not the crystal structure. These features are very common in the POM crystallography.^{2–5}

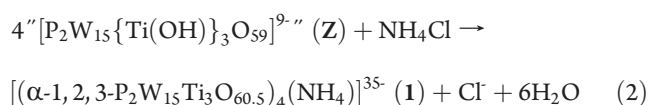
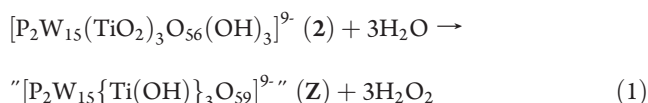
Crystal Data for NH₄Na-1. $\text{H}_{292}\text{N}_{28}\text{Na}_8\text{O}_{332}\text{P}_8\text{Ti}_{12}\text{W}_{60}$: $M = 18036.10$; triclinic, space group $P\bar{1}$; $a = 24.906(7)$ Å, $b = 38.261(11)$ Å, $c = 38.991(11)$ Å, $\alpha = 79.228(5)^\circ$, $\beta = 88.604(5)^\circ$, $\gamma = 87.418(5)^\circ$, $V = 36460(18)$ Å³, $Z = 4$, $D_c = 3.286$ g cm^{-3} , $\mu(\text{Mo K}\alpha) = 19.243$ mm^{−1}. $R_1 = 0.1564$, $wR_2 = 0.2240$ (for all data). $R_{\text{int}} = 0.0856$, $R_1 = 0.0805$, $wR_2 = 0.1846$, $\text{GOF} = 1.023$ (353 990 total reflections, 167 191 unique reflections where $I > 2\sigma(I)$). The maximum and minimum residual density (+11.683 and −5.826 e Å^{−3}) holes were located at 1.01 Å from O6D and 0.26 Å from W1H, respectively.

The main features of the molecular structure of the polyoxoanion (60 tungsten atoms, 12 titanium atoms, 8 phosphorus atoms, 242 oxygen

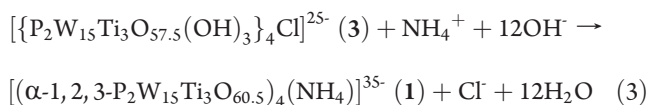
atoms, and 1 encapsulated ammonium cation per formula unit) were clarified. CCDC identification number is 805 517.

RESULTS AND DISCUSSION

Synthesis and Compositional Characterization. A crystalline sample of the nonbridging Dawson tetramer with an encapsulated NH_4^+ cation, $(\text{NH}_4)_{27}\text{Na}_8[(\text{P}_2\text{W}_{15}\text{Ti}_3\text{O}_{60.5})_4(\text{NH}_4)] \cdot \text{ca.} 90\text{H}_2\text{O}$ (**NH₄Na-1**), was obtained in 54% yield by a reaction with NH_4Cl in an aqueous solution at 80 °C for the POM precursor, which was derived by thermal treatment at 200 °C for monomeric triperoxotitanium(IV)-substituted Dawson POM **2**. The composition and molecular formula of **NH₄Na-1** were consistent with complete elemental analysis, including O and Cl analyses, TG/DTA, FTIR spectroscopy, ($^{15}\text{N}\{^1\text{H}\}$, ^{31}P , and ^{183}W) NMR spectroscopy, and X-ray crystallography. The formation of **1** can be represented in eqs 1 and 2. In eq 1, the actual reaction is based on the conversion of the peroxotitanium(IV) species in POM to the hydroxotitanium(IV) species (**Z**) by a reaction with water in an electric furnace at 200 °C and subsequent proton transfer from the Ti–OH–Ti bond in the intra-Dawson unit to the terminal Ti–O group. Equation 2 shows that 4 units of **Z** condense to form the nonbridging Dawson tetramer by encapsulating NH_4^+ cation.

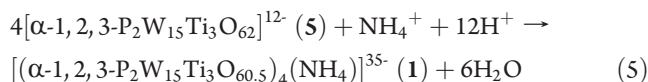
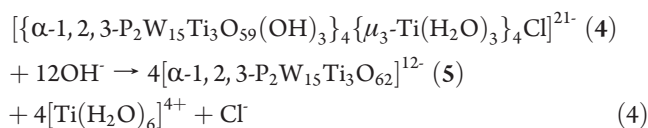


On the other hand, tetramer **1** was also synthesized by the direct exchange of the encapsulated Cl^- ion in the tetrameric POM **3** with the NH_4^+ ion; the ammonium potassium sodium salt of **1**, $(\text{NH}_4)_{24}\text{Na}_7\text{K}_4[(\text{P}_2\text{W}_{15}\text{Ti}_3\text{O}_{60.5})_4(\text{NH}_4)] \cdot \text{ca.} 50\text{H}_2\text{O}$ (**NH₄NaK-1**), was obtained in 45.2% yield by neutralizing the aqueous solution containing **3** with aqueous NH_3 (the initial pH of ca. 2–2.5 was changed to 6.4). The **NH₄NaK-1** was also characterized by complete elemental analysis, TG/DTA, FTIR spectroscopy, and ^{31}P NMR spectroscopy. The formation of **1** from **3** can be represented in eq 3.



Tetramer **1** was also synthesized from a monomeric form of the trititanium(IV)-substituted Dawson POM, $[\alpha\text{-}1, 2, 3\text{-P}_2\text{W}_{15}\text{Ti}_3\text{O}_{62}]^{12-}$ (**5**), in the presence of NH_4Cl under slightly acidic conditions (see Control Experiment 1). It should be noted that the monomeric form **5** of high purity can be derived in good yield only by hydrolysis of the bridging Dawson tetramer with an encapsulated Cl^- ion **4**, but not by any reactions of the nonbridging Dawson tetramer with Cl^- ion **3**. It should be also noted that the monomer **5** as a single species has never been derived from a direct reaction of the trilacunary Dawson species $[\text{P}_2\text{W}_{15}\text{O}_{56}]^{12-}$ with Ti source.^{5c} IR and ^{31}P NMR suggest that the monomer **5** in aqueous solution would be substantially the same as the

hydroxotitanium(IV) species **Z** in eq 1. Such a formation of **1** can be shown in eqs 4 and 5.



Here, it is suggested that the nonbridging Dawson tetramer with an encapsulated Na^+ ion is in-situ-generated in aqueous solution (see Control Experiment 2). The pH-varied ^{31}P NMR spectra of **NaK-3** using aqueous NH_3 showed that some of the bridging oxygen atoms were still protonated in the pH range less than 5.0, but they were completely deprotonated in the pH range greater than 6.0 (up to 8.0). In the synthetic conditions at pH 6.6 using Na_2CO_3 , the edge-sharing oxygen atoms of the Ti–O–Ti bonds are completely deprotonated, and the central cavity becomes highly anionic. The species with an encapsulated Na^+ cation should be formed, because any other cations are not present in this system. Furthermore, the ^{31}P NMR data in control experiment 2 (^{31}P NMR in D_2O , –7.45 and –14.21 ppm) strongly suggest the encapsulation of Na^+ ion.

The samples of **NH₄Na-1** and **NH₄NaK-1** for elemental analysis were dried at room temperature under a vacuum of 10^{-3} – 10^{-4} Torr overnight before analyses. All elements (H, N, Na, P, W, Ti, and O for **NH₄Na-1**, and H, N, Na, K, P, W, Ti, and O for **NH₄NaK-1**) were observed for a total of 99.97% for **NH₄Na-1** and 99.85% for **NH₄NaK-1**, the data of which were consistent with the composition of $(\text{NH}_4)_{27}\text{Na}_8[(\text{P}_2\text{W}_{15}\text{Ti}_3\text{O}_{60.5})_4(\text{NH}_4)] \cdot 17\text{H}_2\text{O}$ and $(\text{NH}_4)_{24}\text{Na}_7\text{K}_4[(\text{P}_2\text{W}_{15}\text{Ti}_3\text{O}_{60.5})_4(\text{NH}_4)] \cdot 15\text{H}_2\text{O}$, respectively. Furthermore, it should be noted that Cl ions were not observed (found <0.1%), revealing that the Cl^- ions are not contained in these complexes. The weight losses observed during the drying before analysis were 6.64% for **NH₄Na-1** and 3.50% for **NH₄NaK-1**, both of which corresponded to ca. 66 and ca. 34 weakly solvated and/or adsorbed water molecules, respectively. Thus, elemental analysis showed a presence of a total of ca. 83 water molecules for **NH₄Na-1** and a total of ca. 49 water molecules for **NH₄NaK-1** under atmospheric conditions. On the other hand, in TG/DTA measurements carried out under atmospheric conditions, a weight loss of 9.18% for **NH₄Na-1** was observed at below 200 °C due to dehydration, with endothermic peaks at 40.7, 64.0, 98.0, 121.9, and 183.0 °C, while that of 5.21% for **NH₄NaK-1** was observed at below 200 °C with an endothermic peak at 57.1 °C (Figures S1 and S2). The former value corresponded to a total of 92 water molecules for **NH₄Na-1**, whereas the latter corresponded to a total of 50 water molecules for **NH₄NaK-1**. Thus, the results by TG/DTA measurements are approximately consistent with those of complete elemental analyses. The formulas were determined on the basis of TG/DTA data at ca. 90 water molecules for **NH₄Na-1** and ca. 50 water molecules for **NH₄NaK-1**.

Solid-state FTIR measurements (Figure 1) of **NH₄Na-1** and **NH₄NaK-1** showed spectral patterns characteristic of the Dawson-type $[\text{P}_2\text{W}_{18}\text{O}_{62}]^{6-}$ POM framework.⁸ The IR spectra of **NH₄Na-1** and **NH₄NaK-1** in the Dawson POM region (1200–400 cm^{-1}) were very similar to that of tetramer **3**, especially with regard to the prominent bands, such as P–O bands (1086 cm^{-1} for **NH₄Na-1**, 1086 cm^{-1} for **NH₄NaK-1**, and 1090 cm^{-1} for **3**),

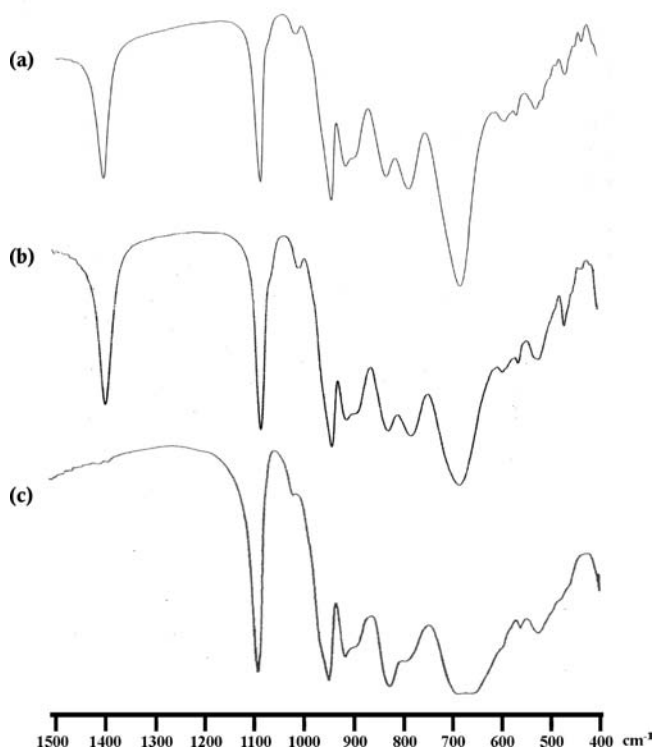


Figure 1. FTIR spectra in the polyoxoanion region ($1500\text{--}400\text{ cm}^{-1}$), measured in KBr disks, of (a) $(\text{NH}_4)_{27}\text{Na}_8[(\text{P}_2\text{W}_{15}\text{Ti}_3\text{O}_{60.5})_4(\text{NH}_4)] \cdot \text{ca.}90\text{H}_2\text{O}$ ($\text{NH}_4\text{Na-1}$) and (b) $(\text{NH}_4)_{24}\text{Na}_7\text{K}_4[(\text{P}_2\text{W}_{15}\text{Ti}_3\text{O}_{60.5})_4(\text{NH}_4)] \cdot \text{ca.}50\text{H}_2\text{O}$ ($\text{NH}_4\text{NaK-1}$) that was obtained by exchange of the encapsulated chloride ion with the ammonium ion (see Experimental Section), and (c) $\text{Na}_{21}\text{K}_4[\{\text{P}_2\text{W}_{15}\text{Ti}_3\text{O}_{57.5}(\text{OH})_3\}_4\text{Cl}] \cdot 70\text{H}_2\text{O}$ (NaK-3), which is the nonbridging Dawson tetramer with an encapsulated chloride ion, as a reference.

the bands assignable to $\text{M}\text{--}\text{O}_{\text{terminal}}$ bonds (943 cm^{-1} for $\text{NH}_4\text{Na-1}$, 944 cm^{-1} for $\text{NH}_4\text{NaK-1}$, and 952 cm^{-1} for **3**), the bands assignable to corner-sharing $\text{M}\text{--}\text{O}\text{--}\text{M}$ bonds (912 cm^{-1} for $\text{NH}_4\text{Na-1}$, 914 cm^{-1} for $\text{NH}_4\text{NaK-1}$, and 918 cm^{-1} for **3**), and the bands assignable to edge-sharing $\text{M}\text{--}\text{O}\text{--}\text{M}$ bonds (831 , 785 cm^{-1} for $\text{NH}_4\text{Na-1}$; 831 , 786 cm^{-1} for $\text{NH}_4\text{NaK-1}$; and 832 cm^{-1} for **3**). The $\text{Ti}\text{--}\text{O}\text{--}\text{Ti}$ vibration bands of inter- and intra-Dawson units were also observed in close positions (687 cm^{-1} for $\text{NH}_4\text{Na-1}$, 688 cm^{-1} for $\text{NH}_4\text{NaK-1}$, and 689 , 662 cm^{-1} for **3**). The $\text{Ti}\text{--}\text{O}\text{--}\text{Ti}$ bands of $\text{NH}_4\text{Na-1}$ and $\text{NH}_4\text{NaK-1}$ were more sharply observed than that of **3**; the $\text{Ti}\text{--}\text{O}\text{--}\text{Ti}$ bands of $\text{NH}_4\text{Na-1}$ and $\text{NH}_4\text{NaK-1}$ were observed as a single peak, while that of **3** was split. This splitting of $\text{Ti}\text{--}\text{O}\text{--}\text{Ti}$ band in **3** would be attributable to coexistence of protonated and deprotonated $\text{Ti}\text{--}\text{O}\text{--}\text{Ti}$ bonds, i.e., $\text{Ti}\text{--}\text{OH}\text{--}\text{Ti}$ bond in the intra-Dawson unit and $\text{Ti}\text{--}\text{O}\text{--}\text{Ti}$ bond of inter-Dawson units. As a matter of fact, the splitting has been observed in independent IR measurements of three different samples such as (689 , 662 cm^{-1}), (689 , 652 cm^{-1}), and (689 , 656 cm^{-1}). On the other hand, all $\text{Ti}\text{--}\text{O}\text{--}\text{Ti}$ bands in $\text{NH}_4\text{Na-1}$ and $\text{NH}_4\text{NaK-1}$ were not split because all $\text{Ti}\text{--}\text{O}\text{--}\text{Ti}$ bonds were deprotonated.

Molecular Structure of 1. The molecular structure of polyoxoanion **1** in $\text{NH}_4\text{Na-1}$, its polyhedral representation, and the partial structure around the central octahedral cavity composed of the $\text{Ti}\text{--}\text{O}\text{--}\text{Ti}$ bonding framework are shown in Figure 2a,b,c, respectively. Selected bond lengths (\AA) and angles (deg) around

the titanium(IV) centers for the Dawson POM unit A in **1** are given Table 1. Other bond lengths (\AA) and angles (deg) in **1** (Table S1) and bond valence sum (BVS) calculations⁹ of the W, P, Ti, and O atoms (Table S2) are shown in the Supporting Information.

The main features of the molecular structure of polyoxoanion **1**, i.e., 60 W atoms, 12 Ti atoms, 8 P atoms, 242 O atoms, and one encapsulated ammonium cation per formula unit, were identified by X-ray crystallography, but the location of some hydrated water molecules and countercations were not determined as the result of disorder. Therefore, the composition and formula of $\text{NH}_4\text{Na-1}$ were determined by complete elemental analysis and TG/DTA analysis.

Structure analysis revealed that the molecular structure of **1** was composed of four " $\text{P}_2\text{W}_{15}\text{Ti}_3\text{O}_{62}$ " Dawson units (designated as A, B, C, and D), which were linked through six intermolecular $\text{Ti}\text{--}\text{O}\text{--}\text{Ti}$ bonds and arranged in approximately T_d symmetry, and one atom occupied the central octahedral cavity; the four Ti_3O_6 faces of the " $\text{P}_2\text{W}_{15}\text{Ti}_3\text{O}_{62}$ " Dawson units occupied four alternate faces of an octahedron. The encapsulated atom was assigned to an N atom (NH_4^+ cation) due to the observed electron density. The encapsulated NH_4^+ cation was confirmed by $^{15}\text{N}\{^1\text{H}\}$ NMR signal at 35.45 ppm of $\text{NH}_4\text{Na-1}$, and the Cl^- ion-free sample was ascertained by complete elemental analysis. The nonbridging Dawson tetrameric structure of **1** was essentially the same as that of the tetramer **3**,^{5b} but the $\text{Ti}\text{--}\text{O}$ bond distances of the $\text{Ti}\text{--}\text{O}\text{--}\text{Ti}$ bonds within the Dawson units in **1** were different from those of **3**. With respect to Dawson unit A, the $\text{Ti}\text{--}\text{O}$ distances of the $\text{Ti}\text{--}\text{O}\text{--}\text{Ti}$ bonds within the Dawson unit in **1** [$1.83(2)\text{--}1.90(2)\text{ \AA}$; average 1.87 \AA] were shorter than those of **3** [$1.888(15)\text{--}1.955(2)\text{ \AA}$; average 1.934 \AA] (see Table 1 and ref 5b). Other bond distances and angles in **1** were in the normal range and were very similar to those in **3**.^{5b} The bond valence sum (BVS) calculations (Table S2) have strongly suggested that all of the oxygen atoms of the $\text{Ti}\text{--}\text{O}\text{--}\text{Ti}$ bonds within the Dawson units are not protonated, i.e., they are due to O^{2-} , but not OH^- . As a result, it appears that the central cavity of **1** becomes highly anionic, and thus, the NH_4^+ cation is encapsulated. On the contrary, all of the 12 oxygen atoms of the $\text{Ti}\text{--}\text{O}\text{--}\text{Ti}$ bonds in **3**, which encapsulate the Cl^- anion, are protonated (see refs 5b and 5d), resulting in the fact that a highly cationic cavity in **3** is constructed and, therefore, the Cl^- anion is encapsulated.

The calculated bond valence sums (BVS),⁹ based on the observed bond distances for Dawson units A, B, C, and D in **1**, were reasonably consistent with the formal valences of Ti^{4+} ($4.020\text{--}4.300$), W^{6+} ($5.874\text{--}6.418$), and P^{5+} ($4.589\text{--}5.075$). The BVS for the O atoms ($1.488\text{--}2.182$), including the oxygen atoms of the $\text{Ti}\text{--}\text{O}\text{--}\text{Ti}$ bonds within the Dawson units (O49, O50, and O51 in each Dawson unit), were also consistent with the formal valence of O^{2-} , indicating that of the all O atoms were not protonated.

From the viewpoint of protonation/deprotonation of the bridging oxygen atoms on the surface, the previously reported tetrameric POM [$(\alpha\text{-}1,2,3\text{-P}_2\text{W}_{15}\text{Ti}_3\text{O}_{57.5}(\text{OH})_3)_4$]^{24,4b} is also discussed here. In 2003, Kortz and co-workers reported a tetrameric POM based on four trititanium(IV)-substituted Dawson subunits with the formula $\text{K}_4(\text{NH}_4)_{20}[\{\text{P}_2\text{W}_{15}\text{Ti}_3\text{O}_{57.5}(\text{OH})_3\}_4] \cdot 77\text{H}_2\text{O}$.^{4b} On the basis of BVS calculations, they indicated that the μ_2 -oxo sites of all three $\text{Ti}\text{--}\text{O}\text{--}\text{Ti}$ bridges within each Dawson fragment are protonated, whereas the μ_2 -oxo sites of the six $\text{Ti}\text{--}\text{O}\text{--}\text{Ti}$ bridges linking the four

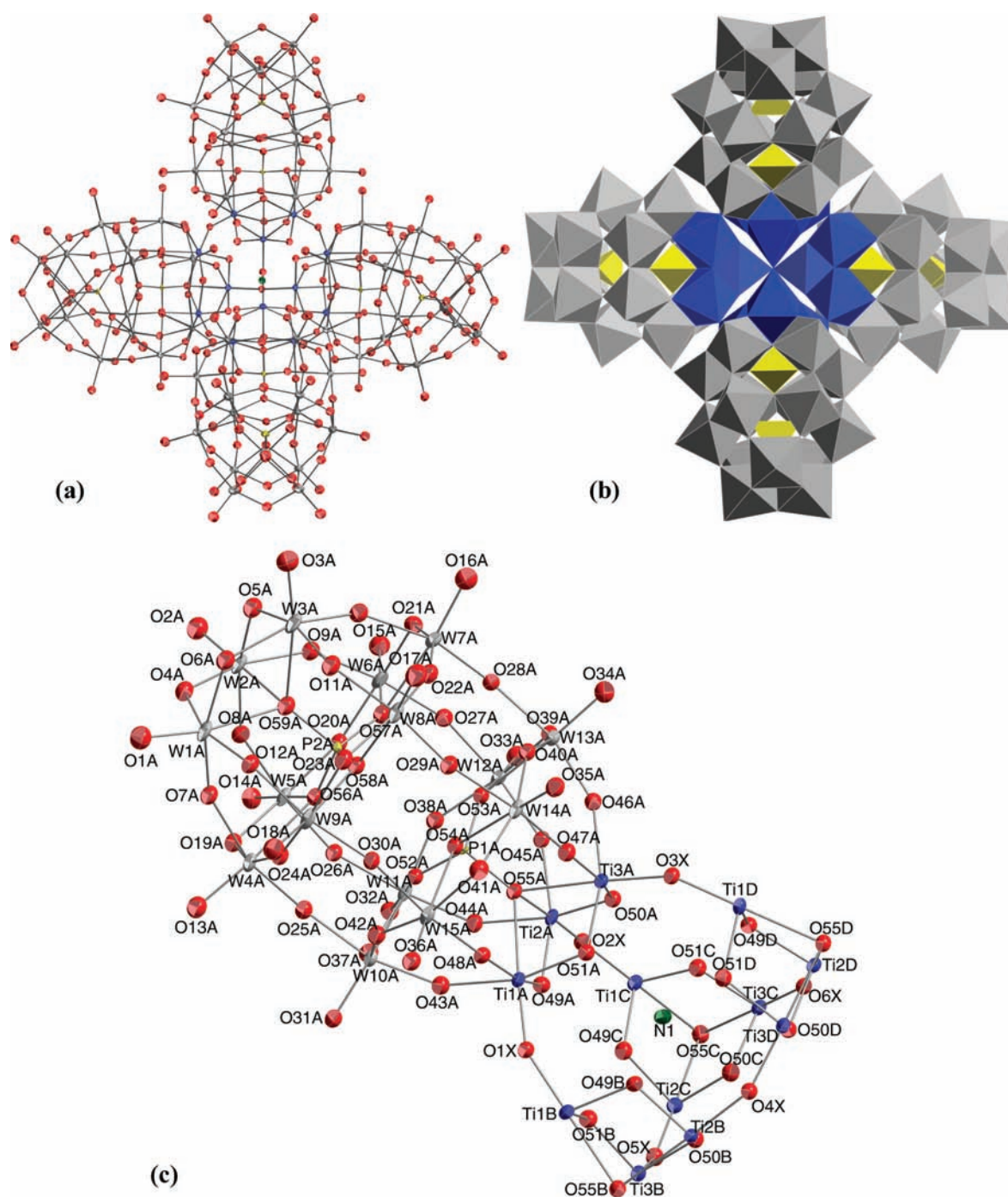


Figure 2. (a) Molecular structure of the polyoxoanion $[(\alpha\text{-}1,2,3\text{-P}_2\text{W}_{15}\text{Ti}_3\text{O}_{60.5})_4(\text{NH}_4)]^{35-}$ **1** in $\text{NH}_4\text{Na-1}$, (b) its polyhedral representation, and (c) the partial structure of the central moiety including the intramolecular and intermolecular Ti–O–Ti bonding framework. Polyhedral representation of the giant “tetrapod” polyoxoanion with approximately T_d symmetry, which is composed of the WO_6 octahedra (gray), the internal PO_4 tetrahedra (yellow), and the TiO_6 octahedra in the Ti_3 cap (blue). The encapsulated anion in the central cavity is hidden.

Dawson fragments to each other are not protonated. As to the protonation sites of the bridging oxygen atoms, their results are reasonable, and the same conclusion was also obtained in regard to our previous compounds, i.e., the nonbridging Dawson tetramer with one encapsulated Cl^- ion, i.e., $[(\alpha\text{-}1,2,3\text{-P}_2\text{W}_{15}\text{Ti}_3\text{O}_{57.5}(\text{OH})_3)_4\text{Cl}]^{25-}$ 3^{5b-d} and the bridging Dawson tetramer with different encapsulated X anions, i.e., $[\{\alpha\text{-P}_2\text{W}_{15}\text{Ti}_3\text{O}_{59}(\text{OH})_3\}_4\{\mu_3\text{-Ti}(\text{H}_2\text{O})_3\}_4\text{X}]^{21-}$ ($\text{X} = \text{Cl}^-$, Br^- , I^- , and NO_3^-).⁵

However, the encapsulated ions in the central cavity are not indicated in the formula.^{4b} The formula apparently shows a compound without any encapsulated ions. Thus, using the CIF file Kortz et al. have deposited, we rechecked the structure analysis and BVS calculation of the bridged oxygen atoms in all Ti–O–Ti bonds. It was confirmed that their compound was the nonbridging Dawson tetramer, but possessing one encapsulated ion in the central cavity. In fact, they analyzed the structure

Table 1. Selected Bond Lengths (Å) and Angles (deg) around the Titanium(IV) Centers for the Dawson-Polyoxoanion Unit A in 1

Ti–O–Ti distances (within Dawson units)		Ti–O–W distances (within Dawson units)			
Ti1A–O49A	1.88(2)	Ti1A–O43A	2.01(2)	W10A–O43A	1.83(2)
Ti2A–O49A	1.90(2)	Ti1A–O48A	1.96(2)	W15A–O48A	1.86(2)
Ti2A–O50A	1.83(2)	Ti2A–O44A	2.00(2)	W11A–O44A	1.85(2)
Ti3A–O50A	1.87(2)	Ti2A–O45A	2.00(2)	W12A–O45A	1.84(2)
Ti3A–O51A	1.86(2)	Ti3A–O46A	2.00(2)	W13A–O46A	1.84(2)
Ti1A–O51A	1.87(2)	Ti3A–O47A	2.02(2)	W14A–O47A	1.82(2)

Ti–Oa distances		Ti–O–Ti Distances between Dawson units	
Ti1A–O55A	2.27(2)	Ti1A–O1X	1.80(2)
Ti2A–O55A	2.30(2)	Ti2A–O2X	1.81(2)
Ti3A–O55A	2.26(2)	Ti3A–O3X	1.82(2)

Angles			
Ti1A–O49A–Ti2A	116.1(12)	Ti2A–O45A–W12A	150.3(13)
Ti2A–O50A–Ti3A	116.6(12)	Ti3A–O46A–W13A	150.7(13)
Ti3A–O51A–Ti1A	114.8(12)	Ti3A–O47A–W14A	150.3(13)
Ti1A–O43A–W10A	149.3(13)	Ti1A–O1X–Ti1B	150.0(14)
Ti1A–O48A–W15A	150.4(13)	Ti2A–O2X–Ti1C	149.2(14)
Ti2A–O44A–W11A	149.5(13)	Ti3A–O3X–Ti1D	148.3(13)

of the compound with one atom (O(O32W)) placed in the central cavity. However, they state in the text of their paper that the atom (O32W) may be an ammonium ion (T_d symmetry) with the same symmetry as a tetrameric POM, although they did not assign an N atom to the structure analysis. In their compound, the description with regard to the central encapsulated ion is not consistent with the formula. Since all of the Ti–O–Ti sites within the Dawson fragments are protonated, the framework constructing the central cavity of the tetrameric POM should be cationic. Thus, the encapsulated ion would be an anionic species, most likely Cl^- , but not a cationic species such as NH_4^+ .

Solution (^{31}P , $^{15}\text{N}\{^1\text{H}\}$, ^{183}W) NMR of 1. The solution ^{31}P NMR spectra of $\text{NH}_4\text{Na-1}$ in D_2O showed a clean two-line spectrum with signals at -7.15 and -14.23 ppm, confirming its purity and single-product nature (Figure 3a). The downfield resonance is assigned to the phosphorus atoms closest to the Ti_3 cap sites, whereas the upfield resonance is due to the phosphorus atoms closer to the W_3 cap in the Dawson units. These chemical shifts of $\text{NH}_4\text{Na-1}$ are different from those of tetramer 3 containing the encapsulated Cl^- anion (-7.6 and -14.0 ppm) (Figure 3d). On the other hand, the ^{31}P NMR spectra of $\text{NH}_4\text{Na-1}$ in 0.1 M HCl aq. (-7.7 and -14.1 ppm) were comparable to that of POM 3 measured in D_2O . The results have suggested that the bridging oxygen atoms on the surface of $\text{NH}_4\text{Na-1}$ in D_2O are deprotonated, while they are protonated under 0.1 M HCl aq conditions. Thus, the encapsulated species in $\text{NH}_4\text{Na-1}$ changes from the cation (NH_4^+) in D_2O to the anion (Cl^-) under HCl conditions. The ^{31}P NMR of $\text{NH}_4\text{NaK-1}$ in D_2O (-7.12 and -14.25 ppm) (Figure 3c) was essentially the same as that of $\text{NH}_4\text{Na-1}$ measured in D_2O .

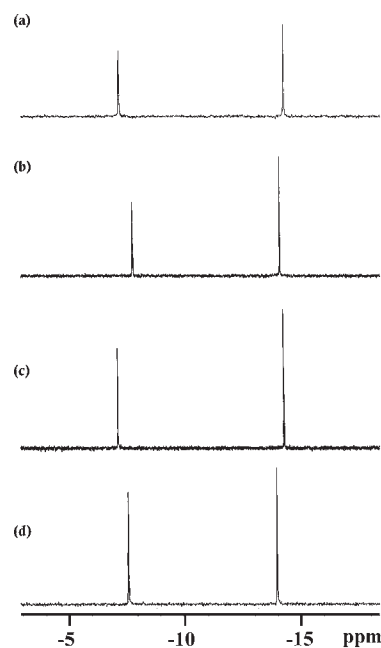


Figure 3. ^{31}P NMR spectra of (a) $(\text{NH}_4)_{27}\text{Na}_8[(\text{P}_2\text{W}_{15}\text{Ti}_3\text{O}_{60.5})_4(\text{NH}_4)] \cdot \text{ca.}90\text{H}_2\text{O}$ ($\text{NH}_4\text{Na-1}$) in D_2O and (b) in 0.1 M HCl aq, (c) $(\text{NH}_4)_{24}\text{Na}_7\text{K}_4[(\text{P}_2\text{W}_{15}\text{Ti}_3\text{O}_{60.5})_4(\text{NH}_4)] \cdot \text{ca.}50\text{H}_2\text{O}$ ($\text{NH}_4\text{NaK-1}$) in D_2O , and (d) $\text{Na}_{21}\text{K}_4[(\text{P}_2\text{W}_{15}\text{Ti}_3\text{O}_{57.5}(\text{OH})_3)_4\text{Cl}] \cdot 70\text{H}_2\text{O}$ (NaK-3) in D_2O as a reference.

The solution $^{15}\text{N}\{^1\text{H}\}$ NMR spectrum of $\text{NH}_4\text{Na-1}$ in D_2O (Figure 4a) was measured using a ^{15}N -enriched sample, which

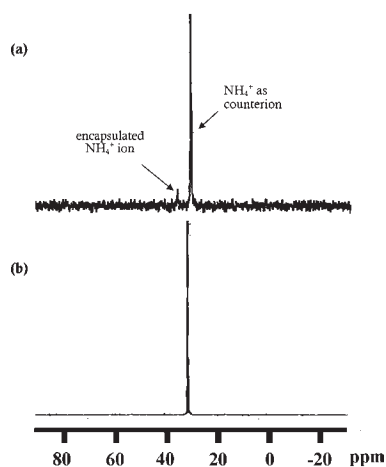


Figure 4. $^{15}\text{N}\{^1\text{H}\}$ NMR spectra in D_2O of (a) the ^{15}N -enriched sample of $\text{NH}_4\text{Na-1}$ prepared using $^{15}\text{NH}_4\text{Cl}$ and (b) $^{15}\text{NH}_4\text{Cl}$ as a reference.

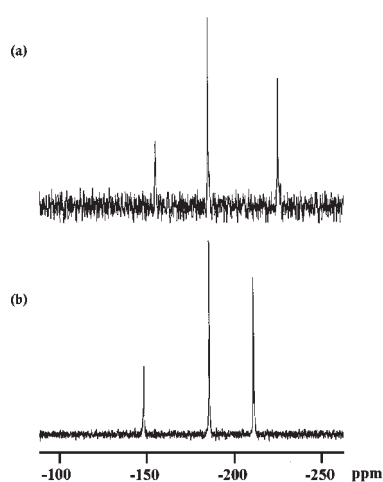


Figure 5. ^{183}W NMR spectra in D_2O of (a) $(\text{NH}_4)_{27}\text{Na}_8[(\text{P}_2\text{W}_{15}\text{Ti}_3\text{O}_{60.5})_4(\text{NH}_4)] \cdot \text{ca.}90\text{H}_2\text{O}$ ($\text{NH}_4\text{Na-1}$) and (b) $\text{Na}_{21}\text{K}_4\{[\text{P}_2\text{W}_{15}\text{Ti}_3\text{O}_{57.5}(\text{OH})_3\}_4\text{Cl}\} \cdot 70\text{H}_2\text{O}$ (NaK-3) as a reference.

was independently prepared using $^{15}\text{NH}_4\text{Cl}$. The $^{15}\text{N}\{^1\text{H}\}$ NMR spectrum of $\text{NH}_4\text{Na-1}$ in D_2O showed a two-line spectrum of 29.89 and 35.45 ppm with integrated intensities of ca. 25:1, due to the counterions and the encapsulated ion, respectively, the larger signal of which should be compared with the $^{15}\text{N}\{^1\text{H}\}$ NMR spectrum in D_2O of the free $^{15}\text{NH}_4\text{Cl}$ alone showing only one peak at 31.56 ppm (Figure 4b). It should be noted that the ^{15}N NMR chemical shift of NH_4^+ as counterion of **1** is not superimposable with that of free NH_4Cl . It is due to the interaction of NH_4^+ counterion with the POM anion, but not from the error in the measurement by the substitution method. These results suggest that the NH_4^+ cation is encapsulated in the central cavity of $\text{NH}_4\text{Na-1}$ in D_2O .

The ^{183}W NMR spectrum of $\text{NH}_4\text{Na-1}$ measured in D_2O showed a three-line spectrum with signals at -154.2 , -184.3 , and -224.5 ppm with integrated intensities of 1:2:2 (Figure 5a) due to the Dawson substructure “[α -1,2,3- $\text{P}_2\text{W}_{15}\text{Ti}_3\text{O}_{62}$] $^{12-}$ ”. It should be noted that the most upfield resonance is much more shifted to a higher field, compared with that of the tetramer **3** (-148.3 , -185.8 , and -211.2 ppm). The difference in the ^{183}W NMR chemical shifts between $\text{NH}_4\text{Na-1}$ and **3** is probably

attributed to whether the oxygen atoms of the Ti-O-Ti bonds are protonated or not. A similar shifting to a higher field was also observed for the mono-Ti-substituted Keggin POM dimer, as previously reported by Kholdeeva et al.³ⁿ

Thus, solution (^{31}P , $^{15}\text{N}\{^1\text{H}\}$, ^{183}W) NMR in D_2O showed that NH_4^+ cation-encapsulating POM **1** is constructed with intramolecular $\text{Ti}-(\mu\text{-O}^{2-})\text{-Ti}$ bonds in Dawson subunits, which is consistent with the solid-state molecular structure revealed by X-ray crystallography. The encapsulating NH_4^+ ion in **1** in D_2O can be exchanged with the Cl^- ion under HCl conditions.

CONCLUSION

The chemistry of the Dawson tetramers composed of four trititanium(IV)-substituted Dawson subunits and their related compounds (**1–5**) has been exhaustively studied here. All ions so far encapsulated in the central cavities of the nonbridging Dawson tetramer and the bridging Dawson tetramer were only anions, i.e., a Cl^- ion for the former^{5b} and Cl^- , Br^- , I^- , and NO_3^- ions for the latter.^{5a,e} In this work, the nonbridging Dawson tetramer encapsulating the NH_4^+ cation, $[(\text{P}_2\text{W}_{15}\text{Ti}_3\text{O}_{60.5})_4(\text{NH}_4)]^{35-}$ **1**, was successfully synthesized by three different methods shown in eqs 1–5 (Results and Discussion), and unequivocally characterized. The possibility of other cation-encapsulating species was also indicated. X-ray crystallography revealed that the framework of the nonbridging tetramer encapsulating the NH_4^+ cation **1** was very similar to that of **3**. The factor determining whether the encapsulated ion in the central cavity is an anion or a cation depends on whether the edge-sharing oxygen atoms of the Ti-O-Ti bonds within the Dawson subunits are protonated or not. Thus, protonation/deprotonation of the $\mu\text{-O}$ atoms in the Ti-O-Ti bonds within the Dawson subunit results in encapsulation of anion/cation in the central cavity of the Dawson tetramer. That is to say, the formation of total $(\text{Ti-OH-Ti})_{12}$ bonds in the Dawson tetramer leads to the cationic character of the central cavity, i.e., anion-encapsulation, while that of total $(\text{Ti-O-Ti})_{12}$ bonds leads to the anionic property of the central cavity, i.e., cation-encapsulation. If a partial protonation such as $(\text{Ti-OH-Ti})_6(\text{Ti-O-Ti})_6$ is possible, the encapsulation of neutral molecules or the formation of an empty cavity may be realized.

The uptake/release of cations by POM-based capsule in solution and the potential of this phenomenon to extend a large variety of cation-transport phenomenon have been described by A. Müller et al.¹⁰ Switching of the encapsulated anion/cation, based on the protonation/deprotonation of the edge-sharing oxygen atoms of the Ti-O-Ti bonds, can be controlled with the pH of the solution, and such a system may be considered as an inorganic model of the ion-transport and ion-channel systems driven by polarization/depolarization of membrane potential in the biological system.¹¹ Synthesis of the tetrameric POMs containing encapsulated cations other than NH_4^+ and Na^+ is in progress.

ASSOCIATED CONTENT

S Supporting Information. Synthesis of the POM precursors. X-ray crystallographic data in CIF format. Selected bond lengths (Å) and angles (deg) around the titanium(IV) centers for the Dawson-POM units B, C, and D for **1**, and average bond lengths (Å) and angles (deg) for the Dawson-POM units in **1** (Table S1). Bond valence sum (BVS) calculations of W, P, Ti, and O atoms for **1** in $\text{NH}_4\text{Na-1}$ (Table S2). TG/DTA of $\text{NH}_4\text{Na-1}$

(Figure S1), $\text{NH}_4\text{NaK-1}$ (Figure S2), and the ammonium sodium salt of **1** derived from the monomer **Na-5** (Figure S3). This material is available free of charge via the Internet at <http://pubs.acs.org>.

AUTHOR INFORMATION

Corresponding Author

*E-mail: nomiya@kanagawa-u.ac.jp

ACKNOWLEDGMENT

This work was supported by a Grant-in-Aid for Scientific Research (C) No. 22550065 from the Ministry of Education, Culture, Sports, Science and Technology, Japan.

REFERENCES

- (1) (a) Pope, M. T.; Müller, A. *Angew. Chem., Int. Ed. Engl.* **1991**, *30*, 34–48. (b) Pope, M. T. *Heteropoly and Isopoly Oxometalates*; Springer-Verlag: New York, 1983. (c) Day, V. W.; Klemperer, W. G. *Science* **1985**, *228*, 533–541. (d) Hill, C. L. *Chem. Rev.* **1998**, *98*, 1–390. (e) Okuhara, T.; Mizuno, N.; Misono, M. *Adv. Catal.* **1996**, *41*, 113–252. (f) Hill, C. L.; Prosser-McCarthy, C. M. *Coord. Chem. Rev.* **1995**, *143*, 407–455. (g) A series of 34 papers in a volume devoted to polyoxoanions in catalysis: Hill, C. L. *J. Mol. Catal.* **1996**, *114*, 1–359. (h) Neumann, R. *Prog. Inorg. Chem.* **1998**, *47*, 317–370. (i) *Polyoxometalate Chemistry from Topology via Self-Assembly to Applications*; Pope, M. T., Müller, A., Eds.; Kluwer Academic Publishers: Dordrecht, The Netherlands, 2001. (j) *Polyoxometalate Chemistry for Nano-Composite Design*; Yamase, T., Pope, M. T., Eds.; Kluwer Academic Publishers: Dordrecht, The Netherlands, 2002. (k) Pope, M. T. In *Comprehensive Coordination Chemistry II*; Wedd, A. G., Ed.; Elsevier Science: New York, 2004; Vol. 4, pp 635–678. (l) Hill, C. L. In *Comprehensive Coordination Chemistry II*; Wedd, A. G., Ed.; Elsevier Science: New York, 2004; Vol. 4, pp 679–759. (m) A series of 32 recent papers in a volume devoted to polyoxometalates in catalysis: Hill, C. L. *J. Mol. Catal. A: Chem.* **2007**, *262*, 1–242. (n) Proust, A.; Thouvenot, R.; Gouzerh, P. *Chem. Commun.* **2008**, 1837–1852. (o) Hasenknopf, B.; Micoine, K.; Lacôte, E.; Thorimbert, S.; Malacria, M.; Thouvenot, R. *Eur. J. Inorg. Chem.* **2008**, 5001–5013. (p) Laurencin, D.; Thouvenot, R.; Boubekour, K.; Villain, F.; Villanneau, R.; Rohmer, M.-M.; Benard, M.; Proust, A. *Organometallics* **2009**, *28*, 3140–3151. (q) Long, D.-L.; Tsunashima, R.; Cronin, L. *Angew. Chem., Int. Ed.* **2010**, *49*, 1736–1758. (r) Dolbecq, A.; Dumas, E.; Mayer, C. R.; Mialane, P. *Chem. Rev.* **2010**, *110*, 6009–6048. (s) Pradeep, C. P.; Long, D.-L.; Cronin, L. *Dalton Trans.* **2010**, 39, 9443–9457. (t) Nomiya, K.; Sakai, Y.; Matsunaga, S. *Eur. J. Inorg. Chem.* **2011**, 179–196.
- (2) (a) Wassermann, K.; Dickman, M. H.; Pope, M. T. *Angew. Chem., Int. Ed.* **1997**, *36*, 1445–1448. (b) Kortz, U.; Hussain, F.; Reicke, M. *Angew. Chem., Int. Ed.* **2005**, *44*, 3773–3777. (c) Hussain, F.; Gable, R. W.; Speldrich, M.; Kogerler, P.; Boskovic, C. *Chem. Commun.* **2009**, 328–330. (d) Ritchie, C. I.; Streb, C.; Thiel, J.; Mitchell, S. G.; Miras, H. N.; Long, D. L.; Boyd, T.; Peacock, R. D.; McGlone, T.; Cronin, L. *Angew. Chem., Int. Ed.* **2008**, *47*, 6881–6884. (e) Thiel, J.; Ritchie, C.; Streb, C.; Long, D. L.; Cronin, L. *J. Am. Chem. Soc.* **2009**, *131*, 4180–4181. (f) Cadot, E.; Pilette, M.-A.; Marrot, J.; Secheresse, F. *Angew. Chem., Int. Ed.* **2003**, *42*, 2173–2176. (g) Gaunt, A. J.; May, I.; Collison, D.; Holman, K. T.; Pope, M. T. *J. Mol. Struct.* **2003**, *656*, 101–106. (h) Pradeep, C. P.; Long, D. L.; Kogerler, P.; Cronin, L. *Chem. Commun.* **2007**, 4254–4256. (i) Mal, S. S.; Kortz, U. *Angew. Chem., Int. Ed.* **2005**, *44*, 3777–3780. (j) Godin, B.; Chen, Y. G.; Vaissermann, J.; Ruhlmann, L.; Verdager, M.; Gouzerh, P. *Angew. Chem., Int. Ed.* **2005**, *44*, 3072–3075. (k) Kim, G.-S.; Zeng, H.; VanDerveer, D.; Hill, C. L. *Angew. Chem., Int. Ed.* **1999**, *38*, 3205–3207. (l) Zhao, J. W.; Zhang, J.; Zheng, S. T.; Yang, G. Y. *Inorg. Chem.* **2007**, *46*, 10944–10946.
- (3) (a) Domaille, P. J.; Knoth, W. H. *Inorg. Chem.* **1983**, *22*, 818–822. (b) Ozeki, T.; Yamase, T. *Acta Crystallogr., Sect. C* **1991**, *47*, 693–696. (c) Knoth, W. H.; Domaille, P. J.; Roe, D. C. *Inorg. Chem.* **1983**, *22*, 198–201. (d) Yamase, T.; Ozeki, T.; Motomura, S. *Bull. Chem. Soc. Jpn.* **1992**, *65*, 1453–1459. (e) Lin, Y.; Weakley, T. J. R.; Rapko, B.; Finke, R. G. *Inorg. Chem.* **1993**, *32*, 5095–5101. (f) Yamase, T.; Ozeki, T.; Sakamoto, H.; Nishiyama, S.; Yamamoto, A. *Bull. Chem. Soc. Jpn.* **1993**, *66*, 103–108. (g) Yamase, T.; Cao, X.; Yazaki, S. *J. Mol. Catal. A: Chem.* **2007**, *262*, 119–127. (h) Nomiya, K.; Takahashi, M.; Ohsawa, K.; Widegren, J. A. *J. Chem. Soc., Dalton Trans.* **2001**, 2872–2878. (i) Nomiya, K.; Takahashi, M.; Widegren, J. A.; Aizawa, T.; Sakai, Y.; Kasuga, N. C. *J. Chem. Soc., Dalton Trans.* **2002**, 3679–3685. (j) Goto, Y.; Kamata, K.; Yamaguchi, K.; Uehara, K.; Hikichi, S.; Mizuno, N. *Inorg. Chem.* **2006**, *45*, 2347–2356. (k) Tan, R. X.; Li, D. L.; Wu, H. B.; Zhang, C. L.; Wang, X. H. *Inorg. Chem. Commun.* **2008**, *11*, 835–836. (l) Hussain, F.; Bassil, B. S.; Bi, L.-H.; Reicke, M.; Kortz, U. *Angew. Chem., Int. Ed.* **2004**, *43*, 3485–3488. (m) Kholdeeva, O. A.; Maksimov, G. M.; Maksimovskaya, R. I.; Kovaleva, L. A.; Fedotov, M. A.; Grigoriev, V. A.; Hill, C. L. *Inorg. Chem.* **2000**, *39*, 3828–3837. (n) Kholdeeva, O. A.; Trubitsina, T. A.; Maksimov, G. M.; Golovin, A. V.; Maksimovskaya, R. I. *Inorg. Chem.* **2005**, *44*, 1635–1642. (o) Hussain, F.; Bassil, B. S.; Kortz, U.; Kholdeeva, O. A.; Timofeeva, M. N.; de Oliveira, P.; Keita, B.; Nadjo, L. *Chem.—Eur. J.* **2007**, *13*, 4733–4742. (p) Al-Kadamany, G. A.; Hussain, F.; Mal, S. S.; Dickman, M. H.; Leclerc-Laronze, N.; Marrot, J.; Cadot, E.; Kortz, U. *Inorg. Chem.* **2008**, *47*, 8574–8576. (q) Ren, Y. H.; Liu, S. X.; Cao, R. G.; Zhao, X. Y.; Cao, J. F.; Gao, C. Y. *Inorg. Chem. Commun.* **2008**, *11*, 1320–1322. (r) Mouri, Y.; Sakai, Y.; Kobayashi, Y.; Yoshida, S.; Nomiya, K. *Materials* **2010**, *3*, 503–518.
- (4) (a) Crano, N. J.; Chambers, R. C.; Lynch, V. M.; Fox, M. A. *J. Mol. Catal. A: Chem.* **1996**, *114*, 65–75. (b) Kortz, U.; Hamzeh, S. S.; Nasser, A. *Chem.—Eur. J.* **2003**, *9*, 2945–2952. (c) Murakami, H.; Hayashi, K.; Tsukada, I.; Hasegawa, T.; Yoshida, S.; Miyano, R.; Kato, C. N.; Nomiya, K. *Bull. Chem. Soc. Jpn.* **2007**, *80*, 2161–2169. (d) Yoshida, S.; Murakami, H.; Sakai, Y.; Nomiya, K. *Dalton Trans.* **2008**, 4630–4638.
- (5) (a) Sakai, Y.; Yoza, K.; Kato, C. N.; Nomiya, K. *Chem.—Eur. J.* **2003**, *9*, 4077–4083. As for the protonation sites within the tetrameric Dawson POMs found with BVS calculations of the oxygen atoms, see also ref 6 cited in ref 5d. (b) Sakai, Y.; Yoza, K.; Kato, C. N.; Nomiya, K. *Dalton Trans.* **2003**, 3581–3586. (c) Nomiya, K.; Arai, Y.; Shimizu, Y.; Takahashi, M.; Takayama, T.; Weiner, H.; Nagata, T.; Widegren, J. A.; Finke, R. G. *Inorg. Chim. Acta* **2000**, *300*–302, 285–304. (d) Sakai, Y.; Kitakoga, Y.; Hayashi, K.; Yoza, K.; Nomiya, K. *Eur. J. Inorg. Chem.* **2004**, 4646–4652. (e) Sakai, Y.; Yoshida, S.; Hasegawa, T.; Murakami, H.; Nomiya, K. *Bull. Chem. Soc. Jpn.* **2007**, *80*, 1965–1974.
- (6) (a) Mbomekalle, I.-M.; Lu, Y. W.; Keita, B.; Nadjo, L. *Inorg. Chem. Commun.* **2004**, *7*, 86–90. (b) Graham, C. R.; Finke, R. G. *Inorg. Chem.* **2008**, *47*, 3679–3686. (c) Contant, R. *Inorg. Synth.* **1990**, *27*, 104–111. (d) Hornstein, B. J.; Finke, R. G. *Inorg. Chem.* **2002**, *41*, 2720–2721. (e) Randall, W. J.; Droegge, M. W.; Mizuno, N.; Nomiya, K.; Weakley, T. J. R.; Finke, R. G. *Inorg. Synth.* **1997**, *31*, 167–185.
- (7) (a) Sheldrick, G. M. *Acta Crystallogr., Sect. A* **1990**, *46*, 467–473. (b) Sheldrick, G. M. *SHELXL-97 Program for Crystal Structure Refinement*; University of Göttingen: Germany, 1997. (c) Sheldrick, G. M. *SADABS*; University of Göttingen: Germany, 1996.
- (8) Rocchiccioli-Deltcheff, C.; Thouvenot, R. *Spectrosc. Lett.* **1979**, *12*, 127–138.
- (9) (a) Brown, I. D.; Altermatt, D. *Acta Crystallogr., Sect. B* **1985**, *41*, 244–247. (b) Brown, I. D.; Shannon, R. D. *Acta Crystallogr., Sect. A* **1973**, *29*, 266–282. (c) Brown, I. D. *Acta Crystallogr., Sect. B* **1992**, *48*, 553–572. (d) Brown, I. D. *J. Appl. Crystallogr.* **1996**, *29*, 479–480.
- (10) (a) Müller, A.; Das, S. K.; Talismanov, S.; Roy, S.; Beckmann, E.; Bögge, H.; Schmidtman, M.; Merca, A.; Berkle, A.; Allouche, L.; Zhou, Y.; Zhang, L. *Angew. Chem., Int. Ed.* **2003**, *42*, 5039–5044. (b) Müller, A.; Rehder, D.; Haupt, E. T. K.; Merca, A.; Bögge, H.; Schmidtman, M.; Heinze-Brückner, G. *Angew. Chem., Int. Ed.* **2004**, *43*, 4466–4470. (c) Ziv, A.; Grego, A.; Kopilevich, S.; Zeiri, L.; Miro, P.; Bo, C.; Müller, A.; Weinstock, I. A. *J. Am. Chem. Soc.* **2009**, *131*, 6380–6382.
- (11) Atkins, P.; Overton, T.; Rourke, J.; Weller, M.; Armstrong, F. *Shriver & Atkins Inorganic Chemistry*, 4th ed.; Oxford University Press: Oxford, U.K., 2006; p 719.